I-18

Dust investigations in TEXTOR: impact of dust on plasma-wall interactions and on plasma performance

A. Litnovsky[1], D. Rudakov[2], S. Bozhenkov[3], R.D. Smirnov[2], S. Ratynskaia[4], H. Bergsåker[4], I. Bykov[4], N. Ashikawa[5], G. De Temmerman[6], Y. Xu[7], S. I. Krasheninnikov[2], W. Biel[1], S. Brezinsek[1], J.W. Coenen[1], A. Kreter[1], M. Kantor[1,6,8], H.T. Lambertz[1], V. Philipps[1], A. Pospieszczyk[1], U. Samm[1], G. Sergienko[1], O. Schmitz[1], H. Stoschus[1] and TEXTOR Team.

[1]*Institut für Energie und Klimaforschung - Plasmaphysik, Forschungszentrum Jülich, Trilateral Euregio Cluster, Association EURATOM- FZ Jülich, D-52425 Jülich, Germany;*

[2]*University of California, San Diego, La Jolla, California 92093-0417, USA;*

[3]*Max-Planck-Institut für Plasmaphysik, Association EURATOM-IPP, Teilinstitut Greifswald, Wendelsteinstrasse 1, 17491 Greifswald, Germany;*

[4]*Royal Institute of Technology (KTH), Association EURATOM-VR, 100 44 Stockholm, Sweden;*

[5]*National Institute for Fusion Science, 322-6 Oroshi, Toki-shi, 509-5292, Japan;*

[6] *Dutch Institute for Fundamental Energy Research (DIFFER), Association EURATOM-FOM, Trilateral Euregio Cluster, Postbus 1207, 3430BE, Nieuwegein, The Netherlands;*

[7]*École Royale Militaire, Association EURATOM-ERM, B-1000, Brussels, Belgium ;*

[8]*Ioffe Physico-Technical Institute, St.Petersburg, Polytechnicheskaya 26, Russia.*

Abstract

Dust will have severe impact on ITER performance since the accumulation of tritium in dust represents a safety issue, a possible reaction of dust with air and steam imposes an explosion

hazard and the penetration of dust in core plasmas may degrade plasma performance by increasing radiative losses. Investigations were performed in TEXTOR where known amounts of pre-characterized carbon, diamond and tungsten dust were mobilized into plasmas using special dust holders.

Mobilization of dust changed a balance between plasma-surface interactions processes, significantly increasing net deposition. Immediately after launch dust was dominating both core and edge plasma parameters. Remarkably, in about 100 milliseconds after the launch, the effect of dust on edge and core plasma parameters was vanished: no increase of carbon and tungsten concentrations in the core plasmas was detected suggesting a prompt transport of dust to the nearby plasma-facing components without further residence in the plasma.

PSI 2012 Keywords: Dust, Impurity transport, tungsten, TEXTOR, ITER

PACs: 52.25.Vy Impurities in plasmas, 52.40.Hf Plasma-material interactions; boundary layer effects, 52.55.Fa Tokamaks, spherical tokamaks

I. Introduction

In future fusion devices like ITER, dust formation imposes a critical issue [1, 2]. The accumulation of tritium in the dust will contribute to the non-desirable in-vessel tritium inventory. The reaction of dust with air due to simultaneous unintentional air ingress and water leak will lead to the explosion hazard. The accumulation of high-Z ions in the core plasma may result in the increase of radiative loss adversely affecting plasma performance. These effects call for immediate efforts in order to understand the mechanisms of dust formation, dust motion and migration and the impact of dust on core and edge plasmas. Joint studies of dust have been conducted in the frame of the International Energy Agency (IEA) – International Tokamak Physics Activity (ITPA) Joint eXperiments Program, and presently involving the DIII-D, TEXTOR, LHD and NSTX facilities and several leading plasma-physics centers.

Dust studies on TEXTOR are aiming at:

- Investigation of dust in fusion plasmas, understanding the physics of dust migration
- Evaluation of the risks and adverse effects on fusion plasma caused by dust and development of risk mitigation strategies

These topics are being experimentally addressed by the intentional introduction of well-defined amounts of pre-characterized dust into edge plasmas and by the subsequent investigations of dust characteristics and an impact of dust on plasma performance. An overview of dust campaigns at TEXTOR 2009-2011 is provided in the paper.

II. Experiment preparation and realization

Dust types

For studies in TEXTOR, several types of pre-characterized dust were selected. Carbon flake-like dust by Toyo Tanso Co.(Japan) was supplied by the DIII-D Team, spherical carbon dust produced by Tokai Carbon Co. (Japan) was shared with the LHD Team, tungsten dust produced by Buffalo tungsten (USA), was identical to that used in MAST. Diamond dust by DiamondTech (Taiwan) was used to study the effect of mobilization of non-conductive dust. The images of dust with the corresponding median size are provided in Fig.1**.** Dust particles had size of 5-10 um which corresponds well to the dust usually collected in fusion devices [3, 4].

Preparations for dust launch

The dust of each type was immersed in ethanol and mixed. The mixture was introduced to the tablet-like dust holders (Fig. 2a) where it dried and formed homogenous and stable dust deposit. Such a technique of dust preparation was successfully applied earlier in DIII-D [5]. The dust holder had a diameter of 25 mm and a spherical cavity of ~ 0.7 mm in its deepest point. Weight measurements of empty dust holders and the holders with dust were performed before and after dust launch allowing for a precise determination of the amount of mobilized dust. Dust holder was mounted in the spherical test-limiter head (Fig. 2a) and the entire assembly was installed into limiter-lock system of TEXTOR [6].

Experimental plan

A scheme of experiments is provided in Fig.2b, showing the top view of TEXTOR torus along with the locations of essential diagnostics used for dust studies. During the exposure in TEXTOR, the dust was mobilized by the direct interaction with TEXTOR plasmas. Immediately after mobilization, the dust was investigated with high-resolution and fast cameras located near the launch locations to evaluate the dust velocity. Edge spectroscopy was deployed to investigate the impurity level around the dust holder. Dust particles were detected by the Thomson scattering

system (TS) [7] which was used to evaluate electron temperature and density during and immediately after the dust mobilization and to determine the size of remaining dust particles and their temperature. The supersonic helium beam [8] was deployed to investigate electron density and temperature in the vicinity of the last closed flux surface (LCFS). Impurity content in the core plasmas was investigated with the ultra-high resolution vacuum ultra-violet (VUV) spectrometer HEXOS [9]. Electron-cyclotron emission (ECE) diagnostic [10] was used to monitor the electron temperature in the core plasma. Dust particles were collected with the aerogel dust collector probe [11]. The detection o dust particles in the aerogels can provide information on dust velocity and amount of dust in the edge plasma.

Mobilization of dust in TEXTOR plasma

Dust holders were driven in the edge plasma behind the last closest flux surface (LCFS). During campaign of 2011, dust holders were even inserted inside the LCFS to ensure guaranteed launch of dust. In all dust campaigns 2009-2011 nearly the same discharge configuration was used for dust studies. TEXTOR was operated at line averaged central density of 2.5×10^{13} cm^{-3}. Neutral beam injection (NBI) with a power of 1.2 MW was usually started one second after the beginning of the discharge. The Thomson Scattering system was activated either during the first 50 ms of the discharge or after 1-1.5 seconds, coincident with NBI start. This was made to evaluate the impact caused by dust at the most expected time of dust launch. The movable aerogel collectors were plunged into TEXTOR plasma using a fast probe drive located in the midplane of TEXTOR (Fig. 2b) and collecting dust particles in outer scrape-off layer (SOL) at the radius r>51 cm. In total, more than 25 launches of dust were made. All types of studied dust demonstrated a similarity during the mobilization: dust was usually mobilized in the very beginning of the discharge, most probably due to plasma load onto the dust holder. An additional, smaller

intensity launch occurred during the start of NBI, due to further increase of the plasma load. The usual amount of mobilized impurities was about 5×10^{19} atoms, the maximum amount did not exceed 1.6×10^{21} atoms.

III. Experimental results and their analyses

Dust in TEXTOR plasma: dust characteristics

Erosion of a dust particle, deposition of impurities on it, ablation of dust along with the main forces acting on the dust particle define its characteristics: dust size and velocity, its temperature and finally, a lifetime of dust in the plasma. For evaluation of dust characteristics the data from several TEXTOR diagnostics was used. These data have provided an input for the DUSTT code. DUSTT is an established code used for dust characterization and evaluation in the fusion plasmas. The code solves the 3D equation of motion of dust particles coupled to the dust charging and dust energy and mass balance models. The detailed description of the DUSTT code is provided in [12, 13]. Forces acting on dust are largely defining its velocity and influence the residence time of dust in fusion plasmas. Among the main forces acting on dust are:

a. Plasma friction force due to flows in plasmas;

b. Gravity force acting on dust due to its mass;

c. Electric force due to the strong electric fields existing in plasmas and acting on the charged dust particle;

d. So-called "rocket" force, due to the non-uniform ablation of the dust by plasma particles.

For evaluation of forces acting on dust in TEXTOR plasma, typical parameters of edge plasmas in the vicinity of the LCFS were used: $N_e=10^{13}$ cm^{-3}, $T_e=60$ eV. A diameter of dust particle was assumed to be 10 μm according to median diameter of pre-characterized dust (Fig. 1). Results of

the evaluation are provided in the table 1 showing that plasma friction force for ~ 1 Mach flow is by far stronger than any other force acting on dust in TEXTOR.

The effect of the rocket force is not provided in the table 1. The rocket force arising from non-uniform ablation of dust grains is very difficult to evaluate due to its random nature associated with irregularities in dust morphology and material properties. The estimates however, show that the rocket force may become important only for few dust particles of largest size mobilized in TEXTOR. Therefore, we will concentrate on the evaluation of dust motion driven by plasma friction force.

With plasma friction as the main force acting on dust, the dust particle of the 10 μm in initial diameter is expected to have the toroidal velocity of order of ~100 m/s in TEXTOR edge plasmas near the LCFS. Estimates correlate well with data from fast cameras located at the bottom of the machine and observing launches of dust from the holder located at the top. Analyses of camera images yield the dust velocity of ~100-120 m/s. However, data from the single camera gives an estimate of velocity projected to the plane of observation, thus providing the lower limit of the actual dust velocity.

Several dust particles were detected implanted in the aerogel dust collectors located as shown in Fig. 2b. Tracks left by the dust particles in these collectors were analyzed and successfully reproduced in the simple laboratory experiment. During this experiment, the dust identical to that used in TEXTOR, was shot at various velocities at the aerogel collector. The resulting tracks of implanted dust particles were compared with those, formed during TEXTOR experiments. The detailed description of the experiment is provided in [14]. The best match of the laboratory-produced and TEXTOR tracks was found at dust velocities in the range of 80-160 m/s which correlates well with the results from fast cameras and with estimates made with the DUSTT code.

Similar velocities of dust particles were observed in DIII-D [5] and NSTX [15] and successfully modeled with the DUSTT code.

An interesting phenomenon was routinely observed during launch of various types of dust in TEXTOR. The motion of dust seems to consist of two independent types: fast motion of the individual dust particles in the toroidal direction with the velocity of ~ 100 m/s as described above and slow motion of the "plume" of dust particles across the toroidal magnetic field with a velocity of ~ 5 m/s. The nature of such a slow motion is presently a subject of investigation. However, such a kind of motion was already observed in TEXTOR during earlier experiments with molten layer [16]. The motion of molten layer was triggered by the thermo-emission current leading to the Lorentz force pushing the layer across the field. Thermo-emission currents are expected to play an important role in dynamics of dust particles [2]. Moreover, charging of dust particles interacting with fusion plasmas occurs within a few nanoseconds of interaction [2] making suitable conditions for thermo-emission current to occur.

Estimates were made for dust in TEXTOR using the DUSTT code with typical plasma parameters along with results of parameter studies [13]. Both carbon and tungsten dust in TEXTOR plasma were expected to ablate strongly being heated by plasma flux. For 10 μm dust particle, the average geometrical reduction rate due to ablation was found to be: 3 mm/s for tungsten and 5 mm/s for carbon dust respectively. These estimates yield to the 2-3 ms lifetime of dust particle in the edge plasma of TEXTOR close to the LCFS, meaning also that both tungsten and carbon particles under these conditions will travel less than 1 m before being completely ablated.

It was possible to detect the ablation of dust with Thomson scattering system [17] located about 20 cm from the dust launch location as shown in Fig. 2b. Dust particles are heated up by plasma and laser beams up to a few thousands of degrees [18]. The particle emits from its surface

thermal radiation which is more intensive than line and Bremsstrahlung radiation of surrounding ablation clouds [18]. Therefore, particle surface temperature is measured from radiation spectra in the assumptions of black body radiation. The size of the particles was calculated from the absolute level of the thermal radiation collected in the observation angle of TS optics taking into account particle ablation during the measurements.

The density of dust particles is measured using thermal radiation detected by the TS spectrometer. The spectrometer collects light from the poloidal cross section of plasma. Since thermal radiation from dust particles well dominated over both plasma light and TS emission, the location and number of dust particles can be detected. The density of dust particles is measured from the statistical analysis of the particles detected along the laser beam. Detailed description of the evaluation of Thomson scattering data is provided in [17]. Analyses of TS data provided an estimate of dust temperature, which for diamond dust was 2500K – 4000K – in the range of temperature required for carbon ablation. The dust size was estimated to be 4 μm at the location of TS system which is roughly 1/2 its initial size (Fig. 1c) due to dust ablation in TEXTOR plasmas. The evaluation of dust concentration immediately after dust mobilization provided a value of 0.5 particle/cm^3 which is about 100 times higher than that measured for intrinsic dust in DIII-D [19].

Impact of dust on plasma performance

Beginning of the discharge, immediately after dust launch

The dependence of electron density N_e and temperature T_e on the vertical diameter of TEXTOR is shown in Fig. 3, as measured at t=60 ms with the TS diagnostic. Distributions were made for the discharge #110269 without dust and the discharge #110272 with a mobilization of diamond dust. Almost two-fold increase and peaking of plasma density occurred immediately after the

launch at t~0. An increase of the temperature was noticed for discharge with dust mobilization (Fig. 3a). Observed evolution of plasma parameters is most likely due to increase of plasma resistance by introduction of dust particles and corresponding better coupling of the power during the ramp-up ohmic phase of the discharge. Distributions of plasma parameters show unambiguously that plasma parameters are dominated by dust during the mobilization and immediately afterwards.

Formed discharge, edge plasmas

The situation changed significantly a hundred of milliseconds after the launch – during the formed discharge. Since the effect of carbon and tungsten dust on plasma performance was nearly identical, the most of analysis will be focused on tungsten dust.

In the edge plasma, radial distributions of electron density and temperature measured with the supersonic He-beam diagnostics are plotted in Fig.4 for a discharge with mobilization of tungsten dust (#110266) and for the reference discharge without dust (#110260). There was only a negligible effect both on T_e and N_e caused by tungsten dust.

Impurity content in the edge plasma was monitored using visible spectroscopy observing the launch location. The respective distributions of the intensity of the WI light at 400.9 nm as a function of the discharge duration was shown for several discharges in Fig. 5. Curve 1 corresponds to the discharge # 115486 when the tungsten dust was launched. Here the significant peak of intensity was noticed at the very beginning of discharge, at t<100 ms and marked in the Fig. 5. The evolution of the intensity of WI light illustrated by curve 1, represents two major contributions:

a) the effect of dust launch in the beginning of discharge (#115485) and (likely) in the beginning of the NBI phase of discharge, at t~1.1 s;

b) the presence of local recycling source – a limiter in the edge plasmas, which influences the WI intensity.

The dependence I_{WI} (t) shown in curve 2, corresponds to the discharge without a launch of tungsten dust (#115487). The comparison of curves 1 and 2 shows, that the effect of dust on edge impurity content can be detected with confidence only in the beginning of the discharge. A slight increase of the intensity at t=1.1 s may also be attributed to the launch of residual mobilizable dust in the beginning of NBI-heating. Finally, the "clean" plasma impurity content, with neither dust mobilization nor local recycling source is shown in curve 3, Fig. 3 (discharge # 115490). From comparison of curves 2 and 3, a strong effect of local recycling source can be inferred. Evolution of plasma parameters and impurity content in edge plasma clearly show, that the effect of dust on the edge plasma is only visible in the very beginning of the discharge and vanishes several hundreds of milliseconds after mobilization.

Similarly, launched dust appeared to cause a weak effect on the core plasma performance during the formed discharge after the NBI-launch. The electron temperature distributions measured with ECE diagnostic are provided in Fig. 6 as measured at the radius R=1.8 m, which is 5 cm towards to the low-field side from the central axis. The distributions of electron temperature measured for the discharge (#110266) accompanied with tungsten dust launch and reference discharge (# 110268) without dust, are nearly identical. Typical distributions of core impurity content measured with HEXOS VUV spectrometer for the discharge (#115485) with W-dust and reference discharge (# 115490) without dust are shown in Fig. 7. The most interesting area is near the wavelength of 5 nm where multiple lines of highly-charged tungsten ions are located. Due to multiplicity of tungsten lines and their proximity to each other, this region is often referred in literature as tungsten "quasi-continuum". A comprehensive description of tungsten VUV lines in the vicinity of quasi-continuum may be found in [20], analyses of quasi-continuum lines for

fusion plasmas are provided in [21]. The comparison of intensity of quasi-continuum lines given in Fig. 7 leads to the conclusion, that the dust caused a negligible effect on core plasma during the formed discharge. Such a weak effect of dust on plasma performance during the formed phase of discharge provokes a question on the strength of the impurity source from the dust. In a simple comparison of the ion source from plasma vs. impurity source from dust, the total number of ions in plasma can be used as an upper estimate of plasma source. This number can be obtained by e.g. multiplying the line-averaged central density by plasma volume of TEXTOR.

The estimate of impurity source from dust can also be done easily using the weight loss measurements. The comparison is provided in table 2. The maximum strength of impurity source from dust is a 213% of that of the plasma source. The strength of tungsten dust source is much lower, corresponding to ~ 3% maximum. It should be noted however, that limitations on tungsten content in burning plasma are by far more stringent than those for carbon. The maximum tolerable tungsten content in ITER is the subject of several analyses [5, 21, 22]. The most recent comprehensive evaluation is provided in [23]. The tolerable tungsten limit presently corresponds to some 10^{-3} percent. The amount of launched tungsten dust in TEXTOR exceeded this limit by several orders of magnitude. Analyses of data from TEXTOR demonstrate that the limit on dust for the safe plasma ignition is by far less critical than the limit for burning plasma initiation.

It is important to compare the amount of injected dust with total amount of impurity atoms eroded during normal plasma operation. An extensive study of erosion and deposition patterns in TEXTOR was undertaken in [24]. Using the maximum measured erosion rates for carbon of $5*10^{16}$ C/cm^2*h and boron of $6*10^{17}$ B/cm^2*h from [24], the conservative estimate of maximum amount of impurities eroded during discharge can be made. According to this estimate, carbon accounts for $2.6*10^{17}$ atoms whereas for boron an amount of launched impurities does not exceed $3.2*10^{18}$ atoms, being still an order of magnitude lower then the weakest source of

impurities from the launched dust. The evaluation of impurity sources show explicitly that in dust introduced to TEXTOR, represented the largest impurity source as compared with natural erosion rates.

Impact of dust on plasma-surface interactions

In dust studies in TEXTOR, the enhanced local deposition of impurities from dust - a reciprocate to the "conversion factor" of the conversion of deposits to dust [25] was routinely observed. Below we provide a quantitative merit of this process using the highest local re-deposition observed with diamond dust. The view of dust holder after two consecutive dust launches is shown in Fig. 8. Total duration of dust launches was less than 2 seconds. Analysis of color fringes on the limiter yielded to the maximum thickness of ~ 400 nm. Therefore, the conservative estimate of the re-deposition rate is larger than 200 nm/sec which is more than 50-times higher, than redeposition rates measured without dust under identical plasma conditions. Enhanced local redeposition provides conditions for the further deposit growth and hence for the subsequent flaking followed by a new dust formation.

Using the weight loss measurements, the amount of launched dust was known with a precision better than 1%. The total amount of launched diamond dust corresponded to $3.8*10^{20}$ atoms. The integrated amount of dust deposited on the holder did not exceed $2.6*10^{19}$ atoms. Therefore, the enhanced re-deposition of dust particles onto nearby PFCs contributes to less than 10% of the overall launched dust. This result coupled with effects of dust on core and edge plasma demonstrates clearly that already several 100 ms after dust launch about 90% of launched dust was transported to the plasma-shadowed areas, like wall structures, diagnostic ports and remote areas without entering the plasma.

IV. Summary and outlook

Known amounts of pre-characterized tungsten and carbonaceous dust particles were mobilized by the direct dust exposure to plasma in TEXTOR. Motion of dust particles along the toroidal magnetic field with the velocity of ~ 100 m/s was estimated using the DUSTT code, with plasma-friction force having the largest impact on dust motion. At the same time, observed motion of the dust with the velocity of ~ 5 m/s across the magnetic field, routinely observed during TEXTOR experiments is yet to be interpreted.

Studies in TEXTOR show that immediately after the mobilization, both core and edge plasma parameters, and impurity mobilizations are dominated by the dust. However, no significant impact on both core and edge plasma parameters was observed hundreds of milliseconds after the launch. The electron temperature and density in the edge plasma and the electron temperature in the plasma core remained unaffected by the dust mobilization despite of significant amount of launched dust accounting for up to 213% and 3% of the total amount of particles in plasma for carbon and tungsten dust respectively. The amount of tungsten dust (3%) is several orders of magnitude higher than the current limitation on tungsten content in ITER (< 0.01%) showing that mobilization of significant amount of dust is unlikely to cause problems with plasma ignition. Weak influence of the launched dust on plasma performance during the formed discharge observed in TEXTOR is inline with the most recent observations made in DIII-D during the launch of dust from modified MiMES midplane manipulator [23].

During dust launches, the increased local redeposition of launched material was routinely observed. The maximum redeposition was measured for diamond dust which was at least 50-fold higher than deposition rates measured without dust. At the same time, the observed enhanced deposition create additional local sources of deposit growth and flaking and at the end – makes conditions for a new dust generation.

Generally, present studies reveal quite a mild effect caused by dust on plasma performance in TEXTOR. The efficiency of dust generation during transient heat and particle loads remain an issue and must be investigated both experimentally and by modeling. Increased local deposition triggered by the dust launch calls for a necessity of evaluation of dust sources.

In future, in order to provide the data for code benchmarking, more defined and simplified conditions for dust introduction into the plasma are necessary. In future studies, the use of dust droppers is envisaged. Dust droppers are supposed to provide reliable and controllable dust injections.

Dust studies are performed on several fusion facilities and a large database on dust interaction with fusion plasmas is obtained. The consolidation of the obtained experience, joint analyses and finally, the joint development of risk mitigation strategies represent an urgent task.

Acknowledgments

Dust studies in TEXTOR were carried out in the frame of multi-machine International Energy Agency (IEA) –International Tokamak Physics Activity (ITPA) Joint eXperiments Program, Task DSOL-21 and bilateral collaborations with partner facilities and institutions. Investigations were partly supported by the tasks WP09-PWI-03-01, WP09-PWI-03-02, WP10-PWI-03-03, WP11-PWI-02-07-01 and WP11-PWI-02-07-02 of the European Fusion Development Agreement (EFDA), Task Force on Plasma-Wall Interactions.

References:

1. G. Federici et al., Nucl. Fusion 41 (2001) 1967;

2. S. I. Krasheninnikov et al., Plasma Phys. and Contr. Fusion 50 (2008) 124054;

3. D. Rudakov et al, Nucl. Fusion 49 (2009) 085022;

4. J. P. Sharpe et al., J. Nucl. Mater. 337–339 (2005) 1000;

5. A. T. Peacock, J. Nucl. Mat. 266-269 (1999) 423;

6. B. Schweer et al. Fus. Sci. and Techn vol. 47 N.2 (2005) 138;

7. M. Kantor et al., Plasma Phys. and Contr. Fusion, 51 (2009) 055002;

8. U. Kruezi et al., "Supersonic Helium Beam Diagnostic for Fluctuation Measurements of Electron Temperature and Density at TEXTOR", accepted to publication in Rev. of Sci. Instr. in 2011;

9. W. Biel et al., Rev. Sci. Instrum. **77**, 10F305 (2006) ;

10. V.S. Udintsev et al., Rev. Sci. Instr. 72 (2001) 359;

11. S. Ratynskaia et al., Nucl. Fusion 49 (2009) 122001;

12. A. Yu. Pigarov et al., Phys. Plasmas 12 (2005) 122508;

13. R.D. Smirnov et al., Plasma Phys. Contr. Fusion 49 (2007) 347;

14. I. Bykov et al., "Time resolved collection and characterization of dust particles moving in the TEXTOR scrape-off layer", these proceedings;

15. A. L. Roquemore et al. J. Nucl. Mater. 363-365 (2007) 222;

16. G. Sergienko et al., J. Nucl. Mater. 363-365 (2007) 96;

17. M. Kantor et al., "Characterization of dust particles in the TEXTOR tokamak with Thomson scattering diagnostic", these proceedings;

18. R. D. Smirnov et al., Plasma Phys. and Contr. Fusion, 51 (2009) 055017;

19. W. P. West, B. D. Bray and J. Burkart, Plasma. Phys. and Contr. Fusion 48 (2006) 1661;

20. R. Neu IPP Garching Report, IPP 10/25 (2003);

21. R. Neu et al. Fus. Eng. and Design 65 (2003) 367;

22. G. Federici et al., J. Nucl. Mater. 313–316 (2003) 11;

23. T. Pütterich et al., Nucl. Fus.50 (2010) 025012;

24. J. von Seggern et al. of J. Nucl. Mater. 313–316 (2003) 439;

25. C. Grisolia J. Nucl. Mater. 390–391 (2009) 53;

26. D. Rudakov, private communications.

Figure captions:

Figure 1: Various types of dust used for TEXTOR experiments: a) carbon flake-like dust, b) carbon spherical dust, c) diamond dust and d) tungsten dust.

Figure 2: Scheme of experiment for investigations of dust in TEXTOR: a) installation a holder with dust on the test limiter) and b) top view scheme of TEXTOR: 1) holder with dust installed on limiter e; 2) Visible spectroscopy of the dust; 3) fast and high resolution cameras; 4) Thomson scattering system; 5) HEXOS XUV spectrophotometer; 6) Fast probe drive equipped with aerogel collectors; 7) ECE diagnostic.

Figure 3: Impact of dust on electron temperature (a) and density (b) immediately after dust launch at t= 60 ms as measured with Thomson scattering system.

Figure 4: Distributions of a) edge density and b) edge electron temperature 1.2 seconds after dust launch, during formed discharge: 1) during the launch of tungsten dust, 2) during the reference discharge without dust mobilization.

Figure 5: Time evolution of WI intensity in the vicinity of dust launch for 1) discharge with W-dust mobilization; 2) discharge without dust and 3) discharge without dust with retracted limiter. Time of dust mobilization is shown with an arrow.

Figure 6: Time evolution of core electron temperature measured with ECE diagnostic for discharges: 1) with dust mobilization (discharge # 110266) and 2) without dust (discharge # 110268).

Figure 7: Core impurity spectra registered at t=1.2 s shown for: 1) discharge with tungsten dust mobilization (# 115485) and 2) discharge without dust (discharge # 115490)

Figure 8: Increased local redeposition of launched diamond dust: a view of the limiter with a dust holder after two dust mobilizations with cumulative duration < 2 s.

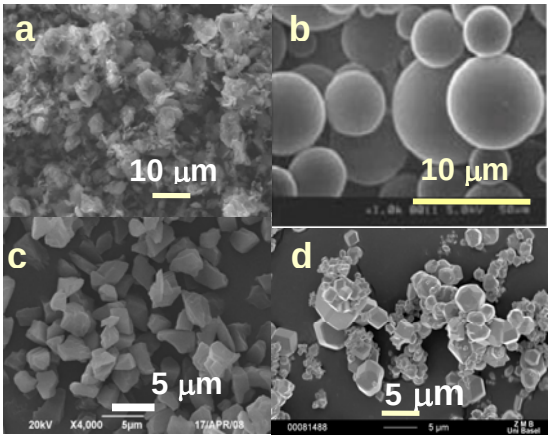

Figure 1.

Various types of dust used for TEXTOR experiments: a) carbon flake-like dust, b) carbon spherical dust, c) diamond dust and d) tungsten dust. Median diameters of each type for each type of dust are given using the data from [3, 4] and the data from the respective manufacturers

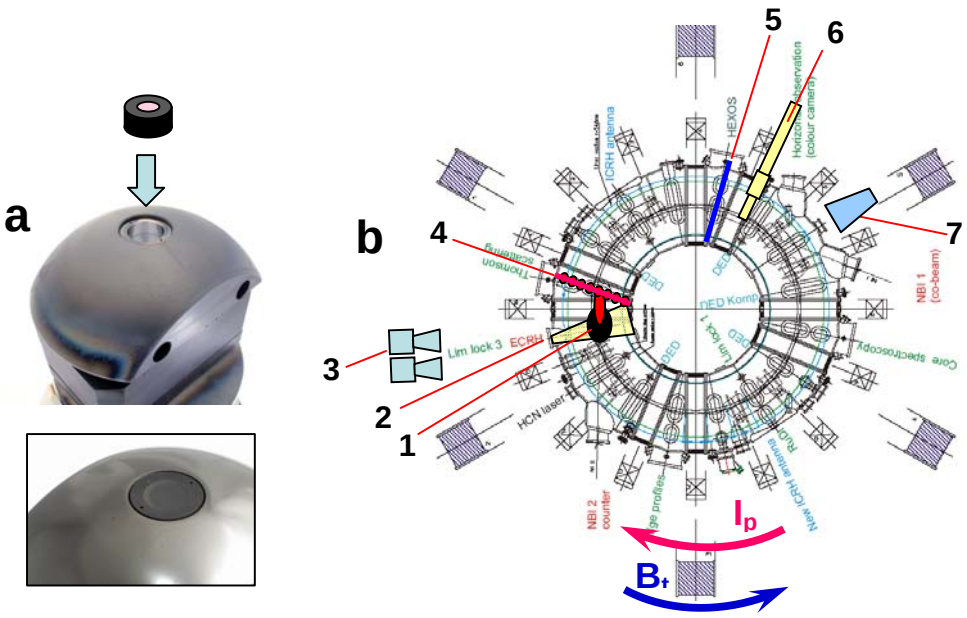

Figure 2.

Scheme of experiment for investigations of dust in TEXTOR: a) installation of a holder with dust on the test limiter) and b) top view scheme of TEXTOR: 1) holder with dust installed on limiter e; 2) visible spectroscopy of the dust; 3) fast and high resolution cameras; 4) Thomson scattering system; 5) HEXOS XUV spectrophotometer; 6) Fast probe drive equipped with aerogel collectors; 7) ECE diagnostic.

Table 1: Forces acting on dust particle

Dust type/Force, N	**Tungsten dust, 10 μm**	**Carbon dust, 10 μm**
Plasma friction force, N	$\sim 7*10^{-8}$	$\sim 7*10^{-8}$
Gravity force, N	$\sim 7*10^{-10}$	$\sim 8*10^{-11}$
Electrical force, N	$\sim 10^{-10}$	$\sim 10^{-10}$

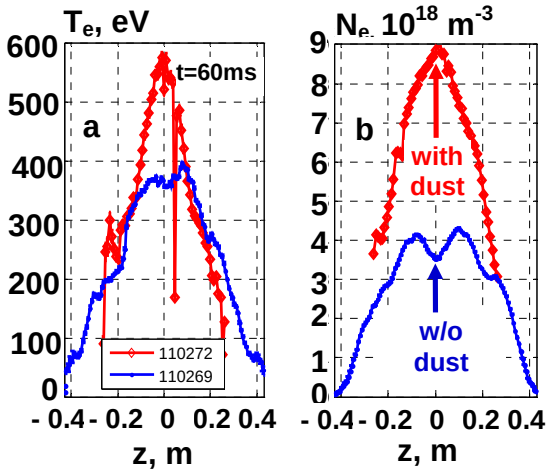

Figure 3.

Impact of dust on electron temperature (a) and density (b) immediately after dust launch at t= 60 ms as measured with Thomson scattering system.

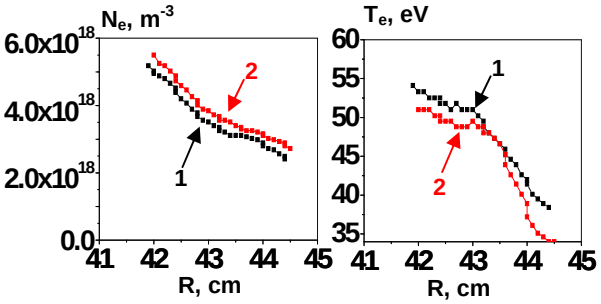

Figure 4.

Distributions of a) edge density and b) edge electron temperature 1.2 seconds after dust launch, during formed discharge: 1) during the launch of tungsten dust, 2) during the reference discharge without dust mobilization

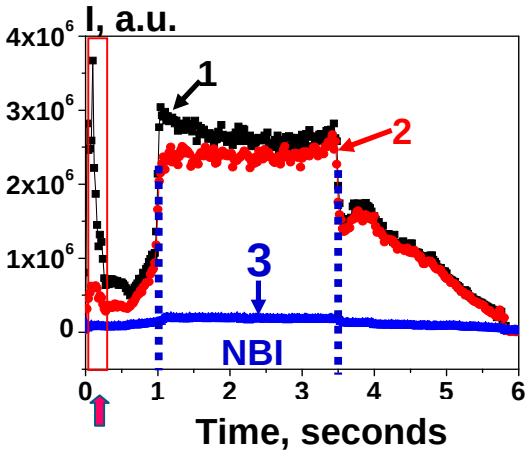

Figure 5.

Time evolution of WI intensity in the vicinity of the dust launch for: 1) discharge with W-dust mobilization (#115485); 2) discharge without dust (#115487) and 3) discharge without dust with retracted limiter (# 115490). Time of dust mobilization is shown with an arrow.

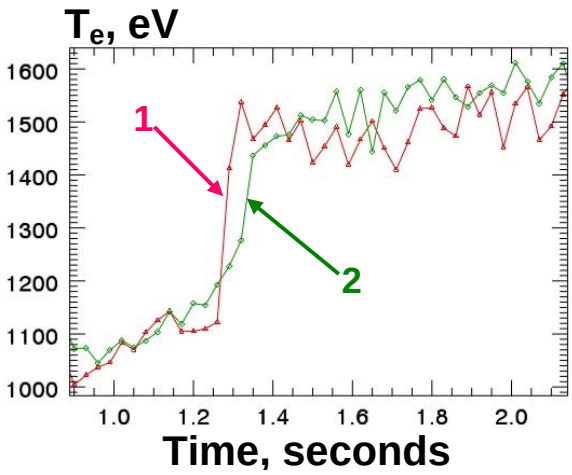

Figure 6.

Time evolution of core electron temperature measured with ECE diagnostic for discharges: 1) with dust mobilization (# 110266) and 2) without dust (# 110268).

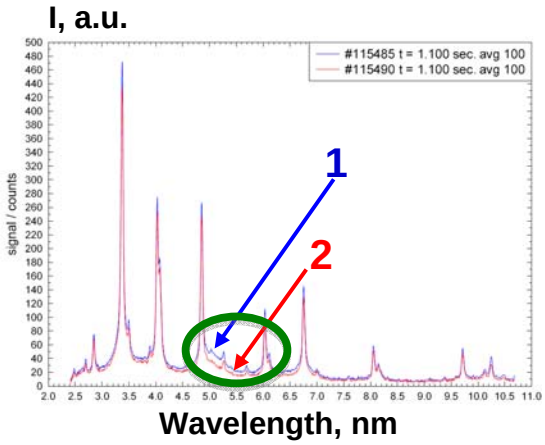

Figure 7.

Core impurity spectra registered at t=1.2 s shown for: 1) discharge with tungsten dust mobilization (# 115485) and 2) discharge without dust (# 115490).

Figure 8.

Increased local redeposition of launched diamond dust: a view of the limiter with a dust holder after two dust mobilizations with cumulative duration < 2 s

Table 2: Plasma source vs. dust source

Plasma source: $N_{plasma} \sim 2*10^{20}$	
Dust source:	
C-dust	**W-dust**
2009: $4.7*10^{20}$ (213 %)	2009: $6*10^{18}$ (3%)
2011: $6.27*10^{19}$ (31%)	2011: $1.75*10^{18}$ (0.91%)